Electrochemical Advanced Oxidation of Carbamazepine: Mechanism and optimal operating conditions

Sara Feijoo, Mohammadreza Kamali, Quynh-Khoa Pham, Azziz Assoumani,
François Lestremau, Deirdre Cabooter, Raf Dewil

Electrochemical Advanced Oxidation of Carbamazepine: Mechanism and optimal operating conditions

Sara Feijoo [a], Mohammadreza Kamali [a], Quynh-Khoa Pham [b,d], Azziz Assoumani [b], François Lestremau [c], Deirdre Cabooter [d], Raf Dewil [a,*]

[a] KU Leuven, Department of Chemical Engineering, Process and Environmental Technology Lab, Jan Pieter de Nayerlaan 5, 2860 Sint-Katelijne-Waver, Belgium
[b] INERIS, Unité Méthodes et Développements en Analyses pour l'Environnement, Rue Jacques Taffanel, 60550 Verneuil-en-Halatte, France
[c] Hydrosciences Montpellier, Univ Montpellier, IMT Mines Ales, IRD, CNRS, 6 Av. de Clavières, 30319 Ales, France
[d] KU Leuven, Department of Pharmaceutical and Pharmacological Sciences, Pharmaceutical Analysis, Herestraat 49, 3000 Leuven, Belgium

ABSTRACT

Effective electrochemical degradation of carbamazepine (CBZ) in water was accomplished with minimal energy and chemical requirements, showing that electrochemical Advanced Oxidation Processes (eAOPs) with a Boron-Doped Diamond (BDD) anode are a promising method for the in situ degradation of contaminants of emerging concern (CECs). The influence of several operating parameters (i.e., pH, temperature and initial anolyte and pollutant concentrations) was determined through the Taguchi optimization method. Optimal conditions corresponded to 1 μM CBZ, pH 2, 30 °C, 10 mM Na_2SO_4 and 50 A m^{-2}, resulting in complete CBZ removal in less than 5 min. Complementary scenarios with different ion species, energy sources and current densities further corroborated the suitability of the optimum. Moreover, they revealed that the optimal conditions were driven by the presence of both SO_4^{2-} and NO_3^- ions in solution. Hence, the optimal degradation results were also attained when replacing HNO_3 by $NaNO_3$, which allowed to operate without prior pH adjustments. The contribution of $^{\bullet}OH$ and $SO_4^{\bullet-}$ radicals was studied through scavenging tests and it was for the first time tentatively ascribed to the Oxygen Evolution Reaction (OER), since the selection of the operating potential influences the type of oxidative species present. Finally, the primary transformation products formed during CBZ degradation under optimal conditions were investigated.

1. Introduction

Driven by the development of more sophisticated analytical techniques, in recent years there has been a notorious increase in international awareness about the presence of contaminants of emerging concern (CECs) in natural water bodies. Their occurrence is largely caused by the limitations of conventional wastewater treatment methods to fully eliminate them [1,2]. Advanced Oxidation Processes (AOPs) have emerged in this context as promising treatments for the degradation of recalcitrant compounds by means of highly reactive radical species, with hydroxyl radicals ($^{\bullet}OH$) being the most prevalent ones [3–5]. Nonetheless, sulfate radicals ($SO_4^{\bullet-}$) have also demonstrated to be effective in the degradation of multiple CECs in various water streams [6,7], showcasing several unique advantages, such as (i) wide redox potential (i.e., 2.5–3.1 V, depending on the pH) [8,9], (ii) reactivity at neutral, acidic and alkaline conditions [10], (iii) longer lifetime than $^{\bullet}OH$ radicals (i.e., approximately 1.5–2 · 10^3 times longer) [7], (iv) fast reaction rates [11] and (v) lower (self-)scavenging effects [12],

which may lead to a higher number of CECs potentially being degraded by $SO_4^{\bullet-}$ [4].

Conventional generation methods for $SO_4^{\bullet-}$ rely on the addition of a precursor such as peroxymonosulfate (PMS, SO_5^{2-}) or peroxydisulfate (PDS, $S_2O_8^{2-}$) that is activated by an external agent (e.g., thermal energy, solar irradiation, ultrasonic irradiation, electricity, low-valent transition metals) [6,8,10]. Few studies have been conducted where precursors are omitted and $SO_4^{\bullet-}$ originates from the sulfate ions (SO_4^{2-}) present in the solution [9,13–15]. To this end, activation of SO_4^{2-} has been attained via electrochemical AOPs (eAOPs), which are considered a promising treatment to degrade CECs for several reasons: (i) high degradation efficiencies and reaction rates can be attained, (ii) no or limited external addition of reactants is needed as the key reaction driver (i.e., electrons) is a clean species (iii) waste and sludge production are reduced compared to other conventional methods, (iv) treatment takes place under mild conditions (i.e., ambient temperature and pressure), (v) safety risks from chemical handling, transportation

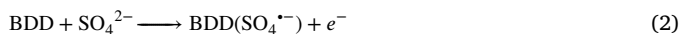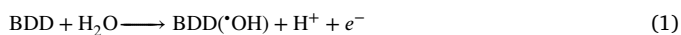|	
AOP(s)	Advanced Oxidation Process(es)
BDD	Boron-Doped Diamond
CBZ	Carbamazepine
CEC(s)	Contaminant(s) of Emerging Concern
CV	Cyclic Voltammetry
eAOPs	Electrochemical Advanced Oxidation Processes
HRMS	High-Resolution Mass Spectrometry
LOD	Limit of Detection
LLOQ	Lower Limit of Quantification
OEP	Oxygen Evolution Potential
OER	Oxygen Evolution Reaction
PDS	Peroxydisulfate
PMS	Peroxymonosulfate
QC	Quality Control
SR-AOPs	Sulfate Radical-based Advanced Oxidation Processes
SR-eAOPs	Sulfate Radical-based electrochemical Advanced Oxidation Processes
TP	Transformation Product
UV	Ultraviolet

and storage are reduced, (vi) environmental footprint associated to their high energy consumption can be compensated by using renewable sources and (vii) integration with other technologies is feasible and often enhances process efficiency [16–18].

A specific electrode material that has been reported to successfully generate $^\bullet$OH and $SO_4^{\bullet-}$ on its surface is Boron-Doped Diamond (BDD) (Eqs. (1) and (2)). BDD electrodes are typically composed of a p-silicon or monocrystalline niobium support with a thin diamond lattice coating doped with boron atoms [19]. This structure showcases high-quality performance in terms of conductivity, potential range, anodic stability, resistance to harsh environments, O_2 over-potential, mechanical durability and lifetime [20,21]; which in turn has proven BDD to be highly effective in CECs degradation for various effluents [22]. Once anodically polarized, the operability of the BDD material is argued to occur by the weak adsorption on its surface (i.e., physisorption) of the different species in solution and by a diverse set of subsequent electron transfer mechanisms, namely four indirect (indicated as 1 to 4 in Fig. 1) and one direct (listed as 5 in Fig. 1) oxidation pathways [23]. It should be noted that indirect mechanisms have been reported more effective than direct oxidation at the anode, not only regarding the CEC degradation but also in terms of $SO_4^{\bullet-}$ formation [22].

$$BDD + H_2O \longrightarrow BDD(^\bullet OH) + H^+ + e^- \qquad (1)$$

$$BDD + SO_4^{2-} \longrightarrow BDD(SO_4^{\bullet-}) + e^- \qquad (2)$$

Carbamazepine (CBZ) is a common anticonvulsant of which approximately 28% is not absorbed by the human body, inevitably entering the sewage system and eventually fresh water reservoirs and seas [26, 27]. Although several studies have been conducted on CBZ degradation via Sulfate Radical-based electrochemical Advanced Oxidation Processes (SR-eAOPs) [14,25], there is still a knowledge gap on the underlying mechanistic phenomena that prevent these techniques from being implemented industrially. Therefore, the main purpose of this study was to further investigate the roles of $SO_4^{\bullet-}$ and $^\bullet$OH radicals for CBZ degradation when generated at the surface of a BDD electrode in an electrochemical cell in order to contribute to the development of wastewater treatments showcasing the "green" advantages of oxidative radicals generated with BDD electrodes (and thus without precursors).
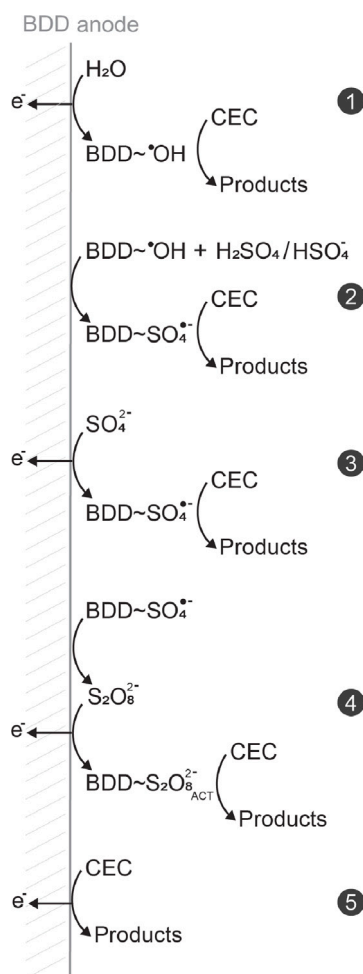

Fig. 1. Postulated phenomena occurring at the BDD anode surface: (1) Indirect CEC oxidation by hydroxyl radicals generated from water electrolysis, (2) Indirect CEC oxidation by sulfate radicals generated from the reaction of hydroxyl radicals with a bisulfate or sulfuric acid medium, (3) Indirect CEC oxidation by sulfate radicals generated from sulfate ions, (4) Indirect CEC oxidation through persulfate generated from the recombination of sulfate radicals and (5) Direct CEC oxidation at the anode. *Source:* Adapted from Diyyapriya and Nidheesh (2021) [22], Song et al. (2018) [14], Chen et al. (2018) [15], Farhat et al. (2018) [24] and Farhat et al. (2015) [25].

As a result, the specific objectives of this research were threefold: (i) to analyze the influence of different operating conditions on CBZ degradation, (ii) to elucidate the underlying degradation mechanism based on the transformation products identified and (iii) to investigate the contribution of different oxidative radicals, namely $SO_4^{\bullet-}$ and $^\bullet$OH.

2. Materials & methods

2.1. Chemicals

High-purity grade carbamazepine ($C_{15}H_{12}N_2O$, CBZ, ≥99%) and acetonitrile (CH_3CN, ≥99.9%, HPLC grade) were purchased from Sigma-Aldrich (Germany). Sulfuric acid (H_2SO_4, 95%) was acquired from VWR Chemicals (France) and potassium hydroxide (KOH, ≥85%) from Carl Roth (Germany). Nitric acid (HNO_3, 65%), tert-butanol (($CH_3)_3COH$, 99.5%), sodium persulfate ($Na_2S_2O_8$, 98%) and sodium nitrate ($NaNO_3$, ≥99%) were purchased from Acros Organics (Belgium). Methanol (CH_3OH, HPLC super grade) was provided by Chem-Lab (Belgium), while sodium sulfate (Na_2SO_4, ≥99%) was purchased from Honeywell (Germany). For the LC-Q-TOF-MS analysis, LC-MS ultra-grade solutions of ammonium acetate ($NH_4C_2H_3O_2$, 7.5 M), acetic acid

(CH_3COOH, glacial) and methanol (CH_3OH, ≥99.9%) were acquired from Sigma-Aldrich (United States), Fisher Scientific (United States) and Honeywell (Germany), respectively. Working solutions were prepared with Milli-Q water purified using a Milli-Q®-Reference system (18 M Ω cm^{-1}) from Merck (Germany).

2.2. Experimental set-up

Degradation experiments were performed in a customized laboratory-scale jacketed electrochemical cell (Fig. A.1) supplied by Redoxme (Sweden), which was made of borosilicate glass and polyether ether ketone (PEEK) material. The cell included a 20 mL cathodic chamber to isolate undesired reduction processes, being divided from the bulk by a cation exchange membrane (Nanoporous PEEK membrane, 50 µm thickness, 25 mm diameter and 20 nm pore size). The solution volume exposed to the degradation was 750 mL. The working electrode consisted of a Boron-Doped Diamond (BDD) coating (polycrystalline, 5-10 µm thick, ~5000 ppm boron doping) on a monocrystalline silicon substrate plate of dimensions $40 \times 80 \times 3$ mm. The counter electrode was a Stainless Steel 317L electrode of dimensions $40 \times 80 \times 0.5$ mm, while the reference electrode selected was Ag/AgCl (+0.210 V vs SHE), placed in the proximity of the BDD electrode. Due to the PEEK holders of the working and counter electrodes, their active surface corresponded to the cathode-facing side and was reduced by approximately 10%. Inter-electrode distance was fixed at 40 mm [14]. Chronopotentiometry experiments were conducted with a potentiostat/galvanostat AUT302N.S PGSTAT302N acquired from Metrohm (Belgium), including a pH/temperature module (pX1000.S) and operated with NOVA software. In general terms, experiments were conducted in batch mode, at room temperature and with constant magnetic stirring at 600 rpm, unless otherwise indicated. To ensure the reproducibility and reliability of the results, experiments were performed at least in triplicate.

Prior to the degradation experiments, the BDD electrode was anodically polarized for 30 min in a 0.1 M H_2SO_4 solution at a constant current density of 100 A m^{-2}, resulting in a stable anode potential of 3.0 ± 0.12 V. Electrochemical degradation of CBZ was then performed in galvanostatic mode by providing constant current densities to the electrochemical cell. At given time intervals, 1 mL samples were collected, filtered with a high-grade syringe filter (CHROMAFIL® Xtra PET, 25 mm diameter, 0.45 µm pore size, Macherey-Nagel, Germany) and subsequently quenched with 500 µL HPLC-grade methanol to prevent further degradation reactions. Scavenging tests were likewise performed, with addition to the reaction matrix of tert-butanol and methanol as scavengers for •OH radicals only and for both •OH and $SO_4^{•-}$ radicals, respectively. The selected molar ratio of both scavengers with respect to CBZ was set to 1000:1, allowing for successful scavenging without affecting the degradation medium [28]. Characterization of the BDD electrode under the operating conditions of interest was carried out by means of Cyclic Voltammetry (CV), which was performed by sweeping from 0 V to +3.0 V (vs Ag/AgCl reference electrode) at a scan rate of 100 mV s^{-1} [22].

Regarding the design of the degradation experiments, four parameters (i.e., CBZ concentration, sulfate anolyte (Na_2SO_4) concentration, pH and temperature) were considered in the comparative assessment of their influence on the degradation kinetics as follows:

- In terms of CBZ concentrations, solutions were prepared at 0.5, 1 and 2 µM. These concentrations were selected because of their similarity to reported CBZ in municipal and urban wastewater (i.e., up to 1.1 µM) [29]. In fact, the presence of CECs in wastewater at low concentrations is a major challenge when implementing AOPs at industrial scale [30], and thus of interest for this research to investigate the performance under realistic conditions.

- Both the anolyte and catholyte consisted of a sodium sulfate (Na_2SO_4) solution. The catholyte concentration was kept at 0.1 M Na_2SO_4 to ensure a suitable conductivity level. In contrast, the anolyte concentration was varied to elucidate its influence on the generation of sulfate radicals. In total, three anolyte concentrations were tested: 1, 5 and 10 mM Na_2SO_4. The rationale behind this selection is two-fold. Firstly, it was desired to operate at sulfate concentrations that would be of similar order of magnitude to those reported in water streams (i.e., up to 6.6 mM and 2.4 mM for surface and groundwater, respectively) [13,25,31]. Secondly, it was desired to operate at sulfate concentrations whose conductivity could ensure a stable current delivery without the need for additional ions, as these could intervene in the degradation reactions. As a result, the current density applied in each case was set to the maximum possible value that would safeguard a constant current for a given natural conductivity. After monitoring the current stability under different conditions (Fig. C.1), the threshold was found to be 25 A m^{-2} per 1 mS cm^{-1} in conductivity, which corresponded to a Na_2SO_4 concentration of approximately 4.5 mM. Therefore, it was decided to set the threshold as 5 A m^{-2} per 1 mM of Na_2SO_4.

- Solution pH was not buffered for any experiment and only initially adjusted with concentrated HNO_3 and KOH to operate at either acidic or alkaline conditions, respectively. In particular, three pH values were selected: 2, 7 (i.e., not adjusted) and 9.

- Both low (i.e., 10 °C) and high (i.e., 30 °C) temperature conditions were tested in addition to ambient values and recreated by means of a circulation cooling water bath system (Witeg, Germany) and a hot water bath (Memmert, Germany), respectively.

2.3. Chemical analysis

The CBZ concentration was monitored using the methodology reported by Yu et al. (2021) with a High Performance Liquid Chromatography instrument (HPLC Agilent 1100, Agilent Technologies, Germany) [32]. The limit of detection (LOD) and the lower limit of quantification (LLOQ) considering the standard error of the calibration intercept were 17.28 and 52.36 µg L^{-1}, respectively. To identify the CBZ transformation products, degradation samples as well as blanks were qualitatively analyzed on an Agilent Infinity 1290 Ultra High Performance Liquid Chromatography (UHPLC) system equipped with a binary pump, a thermostatted autosampler and a heated column compartment, connected to an Agilent 6550 iFunnel Quadrupole Time of Flight Mass Spectrometry (Q-TOF-MS) system (Agilent Technologies, Germany). For the analysis, 5 µL aliquots were injected onto an Acquity UPLC HSS T3 column (2.1×100 mm, 1.8 µm) coupled to an Acquity UPLC HSS T3 VanGuard pre-column (2.1×5 mm, 1.8 µm) from Waters (Ireland) using a gradient program of mobile phases (A) milli-Q water with 1 mM ammonium acetate and 1 mM acetic acid and (B) methanol, at a flow rate of 0.4 mL min^{-1} at 40 °C. The gradient elution program started at 2% B for 0.8 min, followed by an increase up to 40% B in 8.2 min, which was then further increased to 98% B in 11 min and maintained at 98% B for 5 min. Afterwards, the mobile phase composition was returned to the initial conditions in min 0.1 min and kept constant for 4.9 min. The Q-TOF-MS was operated in the Extended Dynamic Range (2 GHz) mode. Ionization was performed in positive electrospray ionization mode using the Dual Agilent Jet Stream Technology, operated at a gas temperature of 200 °C, drying gas flow rate of 15 L min^{-1}, nebulizer pressure of 40 psi and sheath gas temperature and flow rate of 300 °C and 12 L min^{-1}, respectively. The capillary, nozzle and fragmentor voltages were set at 3500, 0 and 365 V, respectively. MS and MS/MS spectra were collected at 2 spectra s^{-1} and 500 ms spectra^{-1}, respectively. Fragmentation was conducted at 10, 20 and 40 eV. In addition, QC pooled samples (i.e., quality-control samples composed of aliquots of all samples included in the sequence) were also analyzed with the LC-QTOF-MS. To ensure the reproducibility of the results, experiments were carried out in triplicate.

2.4. Data analysis

CBZ degradation was modeled under pseudo-first order kinetics and fitted by linear and non-linear regressions, while the influence of different operating parameters was investigated through the Taguchi Method for Design of Experiments. The theoretical background of both data analyses can be found in the Supplementary Material (Section B), where the estimation of the energy consumption parameter is also described. Calculations were performed with RStudio® [33]. Agilent's MassHunter Qualitative Analysis®, MassHunter ProFinder® and MassHunter Personal Compound Database and Library (PCDL) Manager® software were used for the analysis of the transformation products. Peak area normalization based on QC pooled samples was carried out through the MetaboAnalyst platform [34]. Elucidation of the chemical structures corresponding to the detected degradation products based on MS/MS spectra was possible in combination with MetFragWeb online tool [35]. MarvinSketch® was used for drawing, displaying and characterizing chemical structures, substructures and reactions [36].

3. Results & discussion

3.1. Influence of operating conditions on carbamazepine (CBZ) degradation

Given the different parameters and levels of interest, the Taguchi L-9 design was selected (Table A.1). Each experiment was performed in triplicate and the Taguchi S/N analysis (Eq. (3)) was applied to the corresponding reaction rate constants (Fig. 2), which were derived through non-linear regression analysis (Supplementary Material, Section B). Further evaluation of the kinetic models, both regarding residuals analysis and comparison to linear regression results, can be found in the Supplementary Material (Section C).

$$S/N = -10 \log \left(\frac{1}{n} \sum_{i=1}^{n} \frac{1}{y_i^2} \right) \tag{3}$$

Based on the results depicted in Table B.3, the S/N ratio average for the three levels in each of the four parameters was computed (Fig. 3). As defined by the Taguchi Method, optimal levels correspond to those with the highest S/N ratio values. Thus, it can be argued that a combination of the optimal levels will result into a maximized reaction rate constant for CBZ degradation. In this case, the level values of the Taguchi optimum coincide with experiment #7, i.e., pH 2, 10 mM Na$_2$SO$_4$, 30 °C and 1 μM CBZ, ranked in decreasing order of influence on the experimental results. Thus, pH is considered the most influencing factor since it presents the largest S/N range (i.e., 23.2), meaning that a change in its level can result in significant S/N variations. Similarly, initial sulfate anolyte concentration also has a relevant effect, being its S/N range approximately 22.9. On the other hand, varying the temperature or the initial CBZ concentration has a lower impact, as their S/N ranges are approximately 70% narrower than that of the pH. These findings suggest that the treatment performance is more dependent on factors directly related to the generation of oxidative radicals, such as the amount of radical precursors available and the favored radical interactions under different pH conditions.

In addition to the S/N ratio analysis, the relative significance of different parameters plays a major role in determining the effects of the process conditions on the degradation results. Thus, ANOVA analysis was performed with 95% confidence and results are displayed in Table B.3. Given that the corresponding F-values are considerably higher than the critical F-value (i.e., $F_{0.05,1,18} = 4.4139$) and that the p-values are considerably lower than the significance level (i.e., $\alpha = 0.05$), it is possible to reject the null hypothesis that the group means are equal. Therefore, the results obtained are statistically significant. Additionally, ANOVA also enabled the quantification of the parameter contributions, which turned out to be fairly spread across all four process variables. Once again, pH was the most influencing parameter to CBZ degradation kinetics, with a total contribution of 28.4%.

Table 1
Degradation parameters obtained in the experiments carried out to investigate the variability of the Taguchi optimum.

Experiment	Degradation after 60 min (%)	Rate constant (h^{-1})	E$_{EO}$ (kWh m^{-3} order^{-1})
Opt-Na$_2$SO$_4$/HNO$_3$	100.0	55.774	0.019
Opt-Na$_2$SO$_4$/NaNO$_3$	100.0	38.847	0.028
Opt-HNO$_3$	100.0	2.655	0.521
Opt-Na$_2$S$_2$O$_8$	100.0	3.728	0.177
Opt-Na$_2$S$_2$O$_8$/Heat	98.9	2.932	0.000
Opt-Na$_2$SO$_4$	63.4	1.013	0.991
Opt-Na$_2$SO$_4$/Low	11.7	0.123	0.097

The enhanced removal efficiency at acidic pH is also aligned with previous observations [37,38]. However, it should be noted that during the degradation experiments, significant variations in pH were observed in most non-acidic Taguchi experiments, as both the initially alkaline and near neutral pH conditions rapidly evolved towards acidic values (Fig. C.2). It can be argued that this is caused by either (i) the generation of organic acids as transformation products [39,40], (ii) the occurrence of reactions that release protons in solution (Eqs. (1) and Fig. (4)) [14,22,41,42], or (iii) the formation of hydrogen peroxide (H$_2$O$_2$) from the recombination of •OH radicals and its further oxidation (Eqs. (5) and (6)) [22,43,44]. It is also possible that HNO$_3$, which was used to regulate the pH, and its derived nitrate ions (NO$_3^-$) react with SO$_4^{•-}$ radicals (Eq. (7)) or •OH radicals (Eq. (8)) and produce nitrate radicals (NO$_3^•$) [28]. In fact, NO$_3^-$ is a known photosensitizer that can promote the production of •OH and NO$_2^•$ radicals (Eqs. (9) and (10)), leading to indirect photolysis of several CECs, including CBZ [45–47]. This hypothesis is also supported by the degradation rates observed even when no electrochemical treatment was applied and the solution was exposed to natural light (i.e., 16.9% CBZ removal after one hour) (Fig. C.3). Hence, to validate the observed enhanced degradation under acidic conditions, additional experimental scenarios were conducted and are further discussed in the Section 3.2.

3.2. Evaluation of the Taguchi optimum

Based on the Taguchi S/N (Fig. 3) and ANOVA analyses (Table B.3), it was possible to conclude that the optimal conditions that maximize the kinetics of the degradation of CBZ in the studied water matrix are pH 2, 30 °C, 10 mM Na$_2$SO$_4$ anolyte concentration and an initial CBZ concentration of 1 μM. With the Taguchi Method it was possible to predict the optimum value for the reaction rate constant as defined by Eqs. B.5–B.7, where the different prediction components (Table B.4) led to a predicted rate constant of 55.695 ± 2.082 h^{-1}. Additional confirmation replicates of the Taguchi optimum experiment were carried out and the obtained degradation profile is shown in Fig. 5. From the corresponding non-linear regression, the value of the experimental reaction rate constant was found to be 55.774 h^{-1}, which is within its predicted range. Further variations of the Taguchi optimum (referred to as *Opt-Na$_2$SO$_4$/HNO$_3$*) were conducted, as there was a notorious difference in results with respect to all other Taguchi trials and it was desired to confirm the need for the acidic pH conditions. An overview of the conditions of each variation experiment are depicted in Table A.2 and the obtained degradation parameters are shown in Table 1.

In the variation experiment designated as *Opt-HNO$_3$*, no sulfate source was added to the optimal reaction medium. Similarly, in experiment *Opt-Na$_2$SO$_4$*, initial pH was near to neutral values and there was no nitrate source that could participate in the degradation. The rationale behind studying such scenario was that (1) operating at very acidic pH conditions limits the potential of a technology for an industrial roll-out, and (2) avoiding the need for additional chemicals contributes to the economy of the process. Experiment *Opt-Na$_2$SO$_4$/NaNO$_3$* consisted of a variation of the optimum where NaNO$_3$ was used as nitrate source. In this way, it was possible to investigate both the role of pH and the
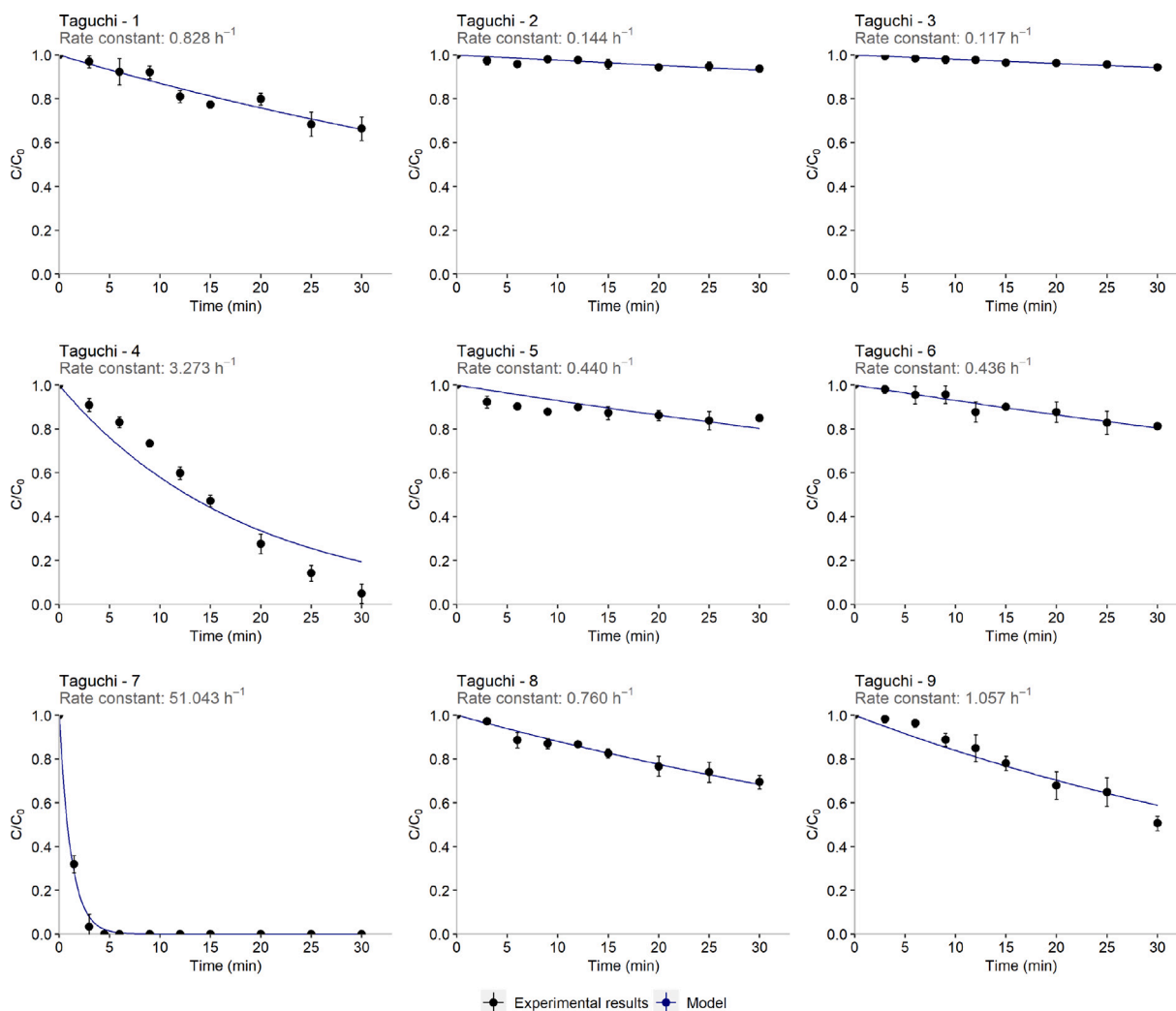
Fig. 2. Derived kinetics of Taguchi L9 design through non-linear regression analysis.

parent species of the potentially generated $NO_3^\bullet$ radicals. As it can be seen in Fig. 6, similar degradation profiles were obtained regardless of the NO_3^- source, and hence, regardless of the initial pH. On the other hand, driving the degradation relying solely on nitrate or sulfate sources (i.e., *Opt-HNO$_3$* and *Opt-Na$_2$SO$_4$*) decreased the reaction rate constant from 55.774 h^{-1} down to 2.655 and 1.013 h^{-1}, respectively. These results demonstrate that the presence of either ions in solution contributed to a reasonable CBZ degradation (over 63% after one hour of treatment), but the synergistic effect of both ions in solution really induced the optimal conditions. Energy-wise, the optimum showed the lowest consumption of electrical energy per order of magnitude (E_{EO}), whereas the highest corresponded to the *Opt-Na$_2$SO$_4$* experiment, being over 50 times more energy-intensive.

To evaluate the relevance of the sulfate source in the optimum, variation experiments consisted of the addition of peroxydisulfate (or persulfate) to the water, as it is a conventional approach in Sulfate Radical-based Advanced Oxidation Processes (SR-AOPs). In such persulfate-driven experiment, 10 mM Na$_2$SO$_4$ was replaced by 5 mM Na$_2$S$_2$O$_8$ as an equivalent source of sulfate ions. Given that persulfate can decompose to H$_2$O$_2$ in strongly acidic solutions [25], the pH was in this case not adjusted. This conventional route was carried out both with and without an electrochemical treatment, which are further referred to as *Opt-Na$_2$S$_2$O$_8$* and *Opt-Na$_2$S$_2$O$_8$/Heat*, respectively. Fig. 7 shows that complete CBZ degradation in a persulfate-based scenario was attained within the one-hour window, although the degradation

kinetics were about 15-fold lower than that of the optimum. In addition, the similarity in results when activating persulfate with and without the electrochemical treatment illustrates that when operating at 30 °C, either approach would be suitable and that its selection could be motivated depending on the associated operating costs or energy consumption.

Based on the results from the CV tests (Fig. C.4), experiment *Opt-Na$_2$SO$_4$* was also performed at a lower current density of 1 A m^{-2} (*Opt-Na$_2$SO$_4$/Low*), corresponding to the conditions below the Oxygen Evolution Potential (OEP). At such low potential, it can be argued that the electrolyte is not fully oxidized, and thus, $\bullet$OH radicals are not the only reactive species in solution [22]. However, Fig. 8 shows significant differences in the degradation profiles between both scenarios and the optimum. This is likely due to a weakened electron transfer at the surface and a subsequently hindered radical formation [38]. In fact, operating at low current densities reduces in this case the reaction rate constant by 99.8%, leading to significantly longer reaction times to attain a suitable removal percentage. In addition, the electrical energy required in such scenario is still greater than that of the optimum.

3.3. Determination of radicals contribution

Scavenging tests were performed to understand the contribution of sulfate and hydroxyl radicals on the overall CBZ degradation in experiments *Opt-Na$_2$SO$_4$* and *Opt-Na$_2$SO$_4$/Low*, as they correspond to different conditions across the Oxygen Evolution Reaction (OER) curve.
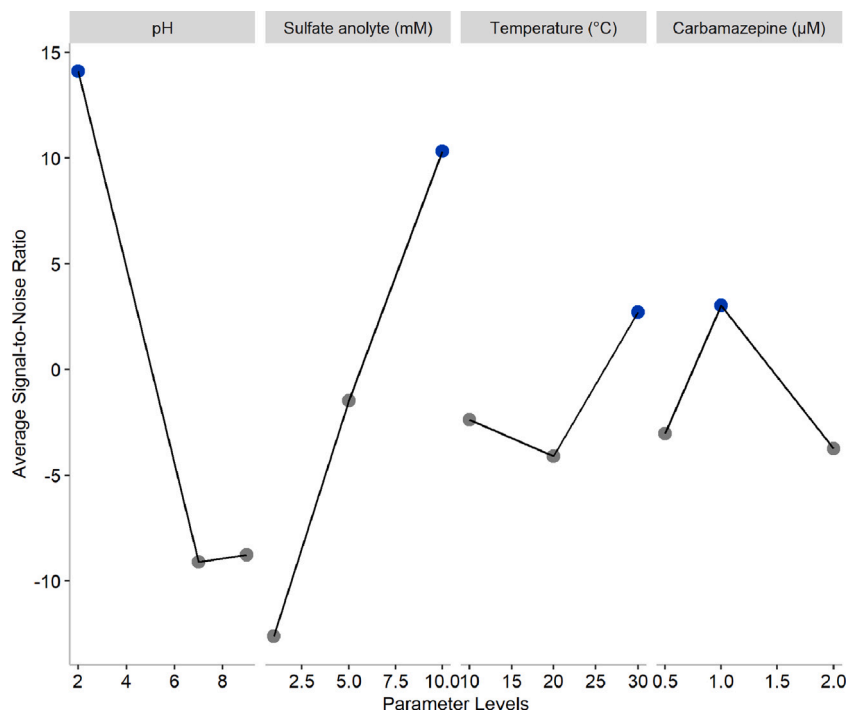
Fig. 3. Average S/N ratios for Taguchi L9 design. The optimal level for each parameter is highlighted as a blue dot.
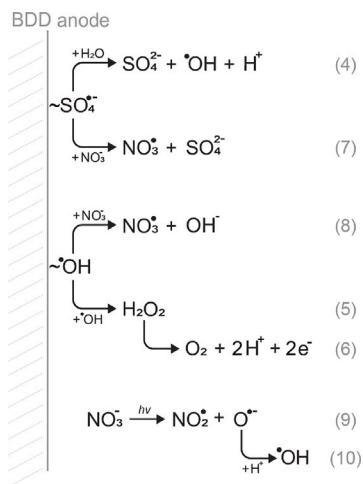

Fig. 4. Postulated reactions that explain the acidic evolution and the role of nitric acid.

This way of indirect identification relies on the addition of radical scavengers to the reaction medium, coupled with a subsequent kinetic analysis (Supplementary Material, Section B) [28,48]. The selected scavengers were tert-butanol and methanol, as the former inhibits $^{\bullet}OH$ radicals and the latter can scavenge both $^{\bullet}OH$ and $SO_4^{\bullet-}$. Fig. 9(a) depicts both scavenging tests applied to experiment *Opt-Na₂SO₄*, where it can be observed that there are perceptible differences in degradation profiles. Such deviations in reaction rate constants led to an estimated contribution of 16% and 84% for $SO_4^{\bullet-}$ and $^{\bullet}OH$ radicals, respectively. In contrast, the scavenging tests with experiment *Opt-Na₂SO₄/Low* (Fig. 9(b)) showed a narrower degree of change among reaction rate constant values, which correspond to a contribution estimation of 1% and 99% for $SO_4^{\bullet-}$ and $^{\bullet}OH$ radicals, respectively. Given that both experiments showcased a dominant presence of $^{\bullet}OH$ radicals, it supports the fact that acidic pH values led to higher degradation efficiencies, as

Table 2
Degradation parameters in scavenging tests.

Experiment	Degradation after 60 min (%)	Rate constant (h^{-1})
Opt-Na₂SO₄/MeOH	32.4	0.4131
Opt-Na₂SO₄/tBuOH	36.1	0.5118
Opt-Na₂SO₄/Low/MeOH	8.5	0.0922
Opt-Na₂SO₄/Low/tBuOH	7.7	0.0924

the redox potential of $^{\bullet}OH$ is at its highest [38]. An overview of the degradation parameters attained is shown in Table 2.

Obtaining such a difference in radical contribution by varying the current density evidences that it is a key parameter in the formation of specific radicals. In fact, the scavenging scenarios entailed either high or low potential (i.e., 2.88 ± 0.17 V and 1.78 ± 0.05 V, respectively), which in turn corresponded to different conditions with respect to the OEP in water (i.e., ~2.5 V). At the BDD, the OER begins with water oxidation that generates $^{\bullet}OH$ radicals (Eq. (1)). At low potential, these $^{\bullet}OH$ radicals recombine to form H_2O_2 (Eq. (5)), which is further oxidized by direct electron transfer towards the formation of $HO_2^{\bullet}$ radicals (Eq. (11)) [49]. At high potential, the process continues, where $^{\bullet}OH$ radicals also react with the electro-generated H_2O_2 (Eq. (12)) and $HO_2^{\bullet}$ radicals play an intermediate role towards the final formation of O_2 (Eqs. (13)–(17)) [49–51]. Therefore, it can be argued that at high potential $^{\bullet}OH$ radicals are dominant, whereas at low potential, $HO_2^{\bullet}$ radicals are also present (See Fig. 10).

When sulfate is involved, at high potential the anolyte is fully oxidized (Fig. C.4) and the recombination of the electro-generated $SO_4^{\bullet-}$ radicals to form persulfate (i.e., $S_2O_8^{2-}$) (Eq. (18)) is observed [22,52,53]. Subsequently, this may trigger a set of reactions where additional $S_2O_8^{\bullet-}$, $O_2^{\bullet-}$ and $SO_4^{\bullet-}$ radicals are formed (Eqs. (19)–(23)) [28,42,51,54,55]. During scavenging tests at high current density with tert-butanol, where $^{\bullet}OH$ radicals were inhibited, a noticeable contribution of $SO_4^{\bullet-}$ radicals was estimated. Thus, it can be argued that the degradation of CBZ occurs thanks to the presence of free $SO_4^{\bullet-}$ and/or $S_2O_8^{\bullet-}$ radicals, as $O_2^{\bullet-}$ is likely to participate in the OER. In contrast, at low potential the sulfate anolyte is not fully oxidized. Thus, the formation
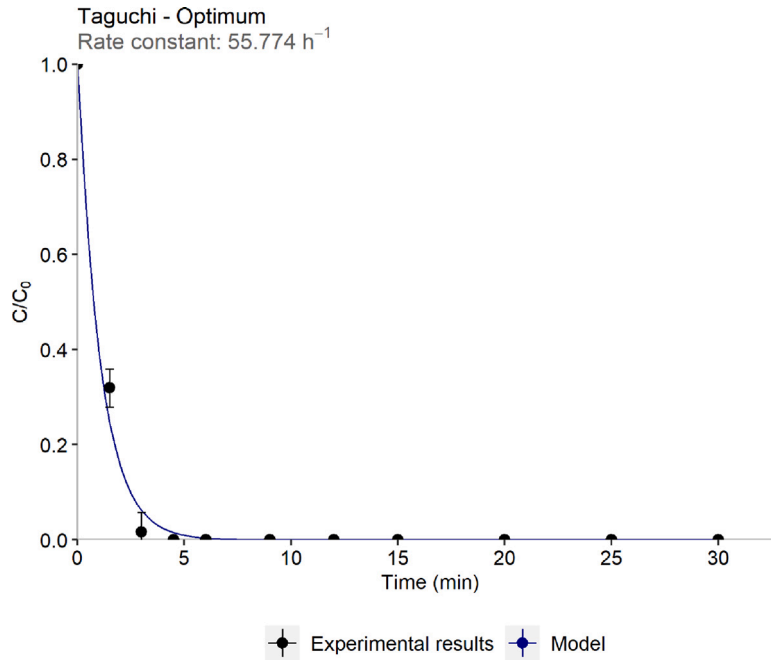
Fig. 5. Additional replicates on the degradation of CBZ under the Taguchi optimum: pH 2, 10 mM Na_2SO_4, 30 °C, 1 µM initial CBZ and 50 A m^{-2}.
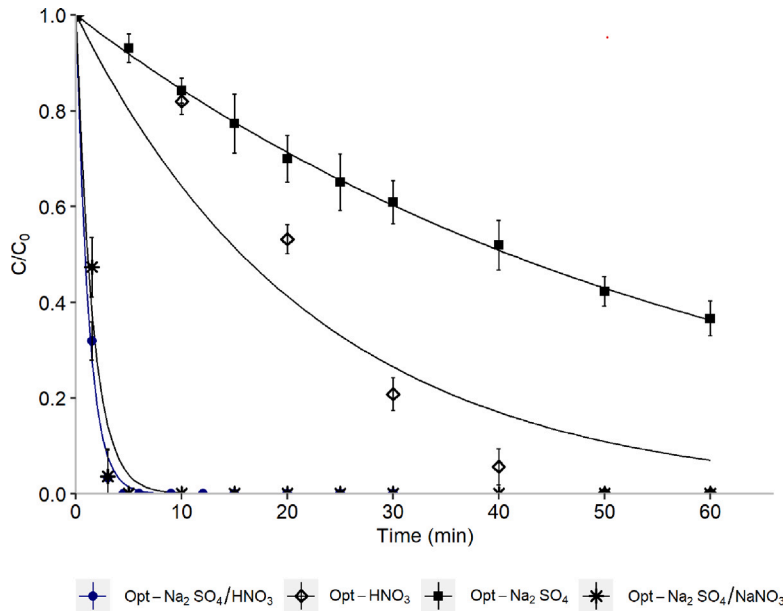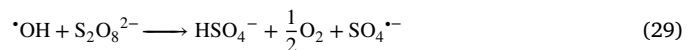

Fig. 6. Optimum variation experiments to investigate the influence of sulfate and nitrate ions.

of $S_2O_8^{2-}$ is not observed and its subsequent reactions are limited. In addition, at low potential, $HO_2^{\bullet}$ radicals originating from the OER may act as a scavenger of $SO_4^{\bullet-}$ radicals (Eq. (24)) [54] as well as non-oxidized water molecules may lead to the generation of $^{\bullet}OH$ radicals (Eq. (25)) [22,42,51], which are eventually scavenged by tert-butanol. As a result, the occurrence of both these reactions and the absence of additional radicals deriving from the co-generation of persulfate, brings a plausible explanation to the lower $SO_4^{\bullet-}$ radical contribution observed at low current density (See Fig. 11).

Even though these hypotheses encourage to operate at higher current densities to avoid a possible scavenging of sulfate radicals and promote their participation in the degradation of CBZ as well as attain faster kinetics, they are not directly scalable to a non-scavenged scenario, where additional reactions can take place (Eqs. (26)–(32)) [22,

28,42,50–52,54,55]. In fact, Eqs. (27)–(30) show that $^{\bullet}OH$ radicals can play a key role in the formation of $SO_4^{\bullet-}$ radicals. Given that the investigated scavenging scenarios promoted $^{\bullet}OH$ scavenging, the formation of $SO_4^{\bullet-}$ could have been equally hampered in both, with the detected $SO_4^{\bullet-}$ radicals only originating at the anode. Consequently, the precise nature and origin of the radicals participating in the degradation of CBZ as well as their degree of involvement needs to be further elucidated.

$$SO_4^{\bullet-} + OH^- \longrightarrow SO_4^{2-} + {}^{\bullet}OH \tag{26}$$

$${}^{\bullet}OH + SO_4^{2-} \longrightarrow OH^- + SO_4^{\bullet-} \tag{27}$$

$${}^{\bullet}OH + HSO_4^- \longrightarrow H_2O + SO_4^{\bullet-} \tag{28}$$

$${}^{\bullet}OH + S_2O_8^{2-} \longrightarrow HSO_4^- + \frac{1}{2}O_2 + SO_4^{\bullet-} \tag{29}$$
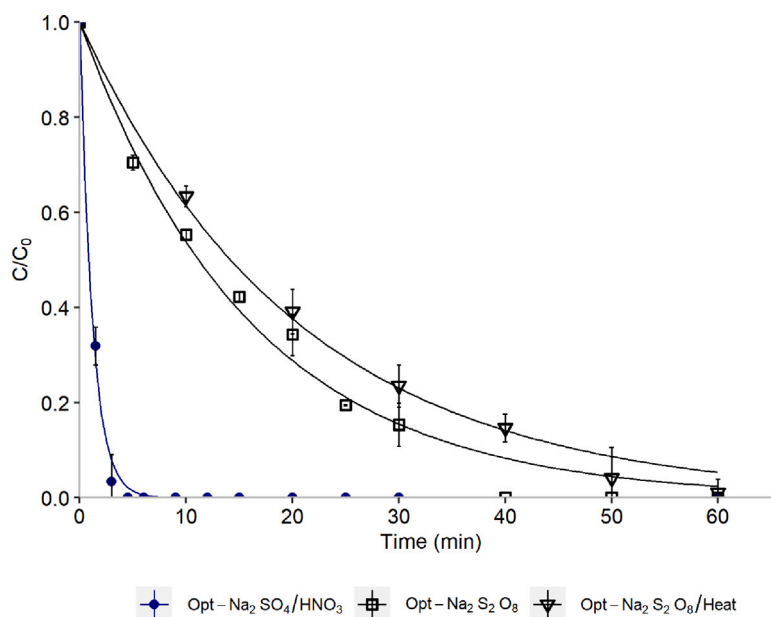
Fig. 7. Optimum variation experiments for comparison with persulfate-driven treatments.

Fig. 8. Optimum variation experiments to evaluate different current densities in a sulfate-containing medium.

$$^\bullet OH + S_2O_8{}^{2-} \longrightarrow OH^- + S_2O_8{}^{\bullet-} \qquad (30)$$

$$^\bullet OH + SO_4{}^{\bullet-} \longrightarrow HSO_4{}^- + \frac{1}{2}O_2 \qquad (31)$$

$$^\bullet OH + SO_4{}^{\bullet-} \longrightarrow HSO_5{}^- \qquad (32)$$

3.4. Elucidation of CBZ transformation products during Taguchi optimum

The degradation mechanisms of CBZ have been extensively investigated in multiple AOPs as well as mediated by various oxidative species. An overview of transformation products previously reported can be found in Table D.1. In this study, the focus was on identifying transformation products that are formed during the Taguchi optimum experiment, given the novelty of these conditions. Thus, a non-targeted screening by means of HRMS analysis was conducted within the time window in which carbamazepine is fully depleted (i.e., up to 5 min). Based on the MS results, transformation products were detected based on their exact mass, m/z value and retention time. In addition, experimental peak areas were normalized with respect to the peak area of carbamazepine before degradation. Only the transformation products that (i) were not detected in the initial sample, (ii) appeared in all experimental replicates when detected at later times, (iii) exhibited a fold-change at any sampling time equal or higher than 2 [56] and (iv) showed a maximum relative peak area of at least 0.2% with respect to the initial CBZ, were considered as relevant and are reported here. As a result, 10 transformation products were detected, which can be argued to be intermediates of reaction due to their bell-shape profile (Fig. 12) and complete disappearance after 20 min of treatment (data not shown). The most abundant transformation products were the intermediates with exact mass 356.1489 g mol^{-1}, 320.0778 g mol^{-1} and 268.0857 g mol^{-1}.

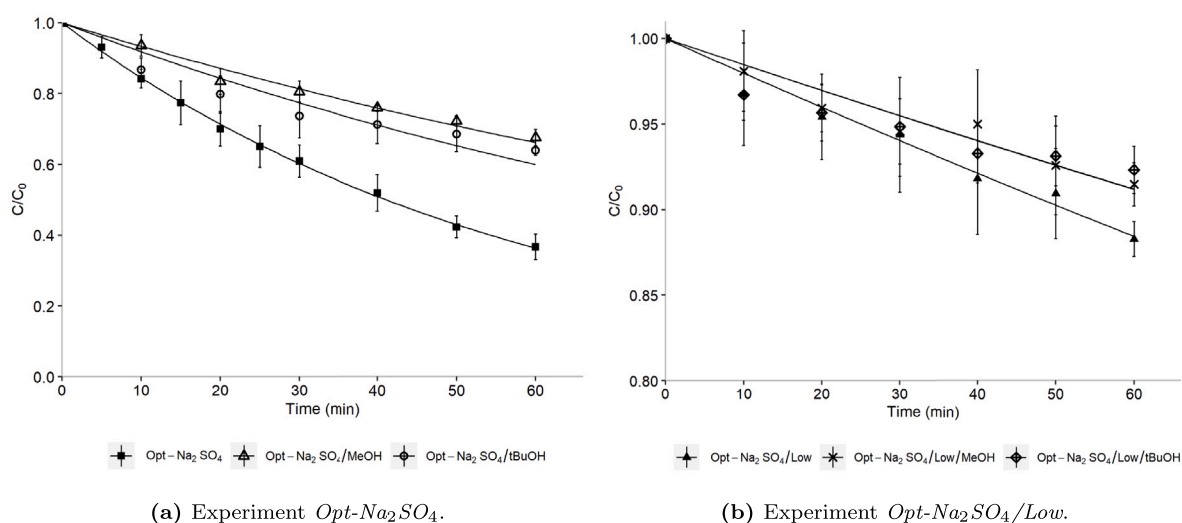**(a)** Experiment $Opt\text{-}Na_2SO_4$.

(b) Experiment $Opt\text{-}Na_2SO_4/Low$.

Fig. 9. Scavenging tests consisting in the addition of methanol (i.e., MeOH) or tert-butanol (i.e., tBuOH) to experiments **(a)** $Opt\text{-}Na_2SO_4$ and **(b)** $Opt\text{-}Na_2SO_4/Low$.
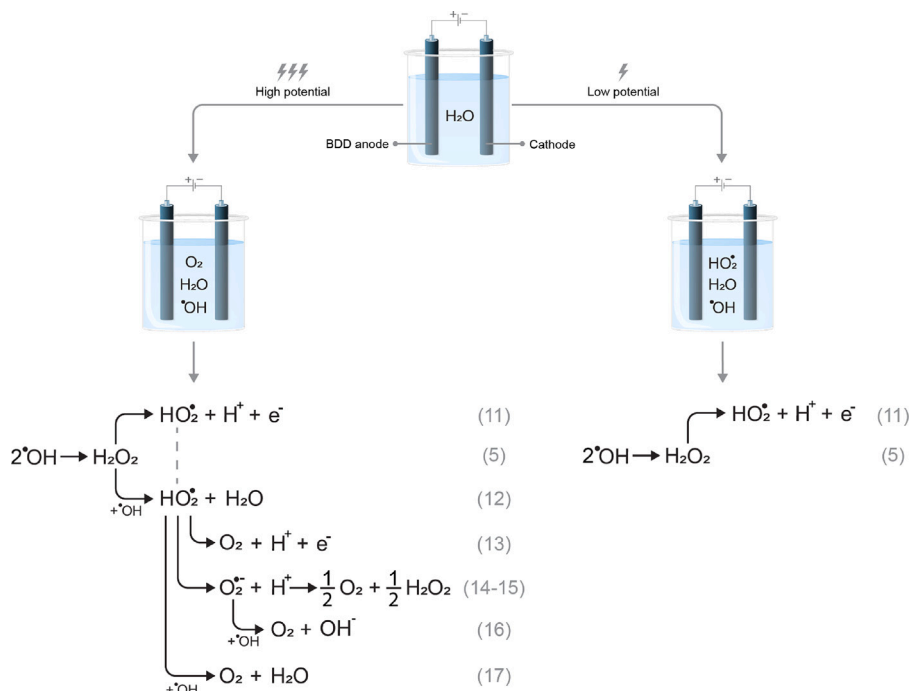

Fig. 10. Oxygen Evolution Reaction (OER) at high and low potential.

A tentative identification of the chemical structures corresponding to these 10 transformation products was performed, out of which several feasible structures were proposed for 8 transformation products (Fig. 13 and Table 3). The elucidation of these structures relies on a comparative analysis with database information for the MS/MS spectra obtained after the targeted fragmentation of each compound in the samples showcasing the highest peak intensity values. Detailed information on MS/MS spectra for each proposed structure can be found in the Supplementary Material (Section D). The final selection of suitable chemical structures was based on (i) a qualitative and quantitative analysis of the fragments matched, (ii) the validation that their retention time and expected polarity (i.e., logP value) were in agreement to those of CBZ as reference (RT: 13 min, logP: 2.77), and (iii) their structural resemblance to the parent compound. As a result, a total of 25 possible chemical structures were proposed. The 19 structures assigned to the transformation products ranging from 195.0687 g mol^{-1} to 285.1009 g mol^{-1} appear to be more likely, as

they met all 3 selection requirements. For further structural confirmation of these compounds and possible evaluation of their toxicity implications, their MS/MS spectra should be validated with those of reference standards as well as it would be recommended to investigate their possible evolution towards secondary transformation products, given that they were eventually eliminated within the lapse of time under study. In addition, it can be argued that some of these transformation products are novel compounds and therefore have not been yet characterized and included in the databases of reference. Therefore, in such cases additional research would be required to consolidate their identification.

3.5. Scale-up and future research recommendations

This study has shown that the BDD electrochemical Advanced Oxidation Process is a promising method for the degradation of CECs in
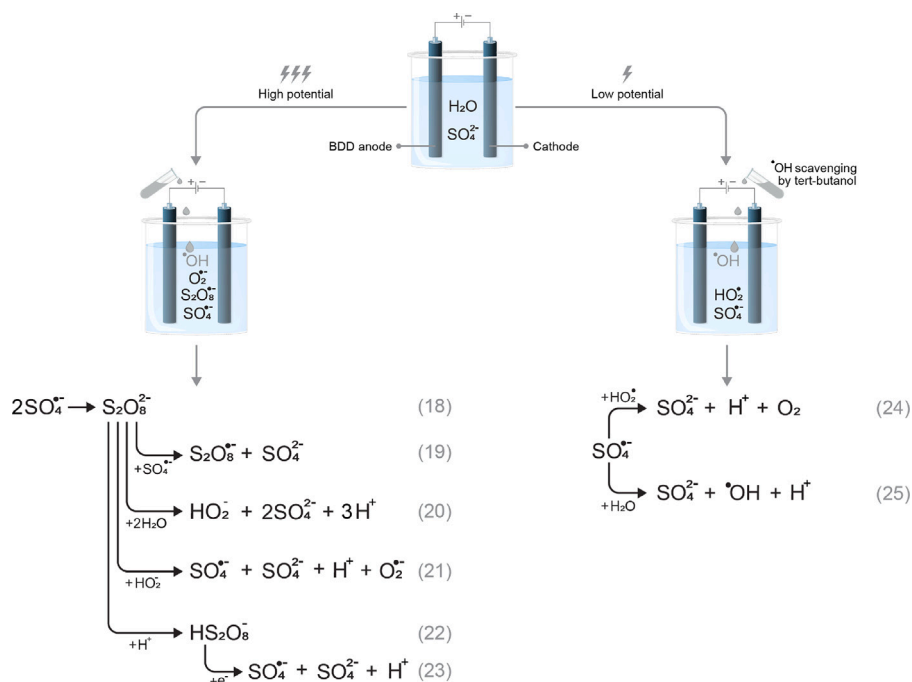
$$2SO_4^{\bullet-} \rightarrow S_2O_8^{2-} \quad (18)$$

$$\xrightarrow{+SO_4^{\bullet-}} S_2O_8^{\bullet-} + SO_4^{2-} \quad (19)$$

$$\xrightarrow{+2H_2O} HO_2^- + 2SO_4^{2-} + 3H^+ \quad (20)$$

$$\xrightarrow{+HO_2^-} SO_4^{\bullet-} + SO_4^{2-} + H^+ + O_2^{\bullet-} \quad (21)$$

$$\xrightarrow{+H^+} HS_2O_8^- \quad (22)$$

$$\xrightarrow{+e^-} SO_4^{\bullet-} + SO_4^{2-} + H^+ \quad (23)$$

$$SO_4^{\bullet-} \xrightarrow{+HO_2^{\bullet}} SO_4^{2-} + H^+ + O_2 \quad (24)$$

$$\xrightarrow{+H_2O} SO_4^{2-} + {}^{\bullet}OH + H^+ \quad (25)$$

Fig. 11. Sulfate radical-based reactions involved in scavenging tests with tert-butanol.
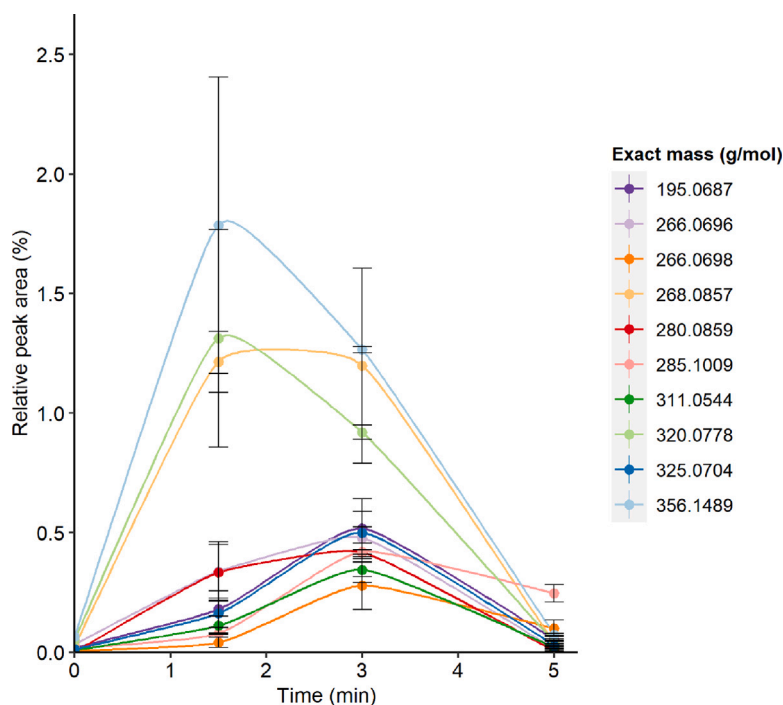

Fig. 12. Detected CBZ transformation products (expressed in terms of exact mass) during Taguchi optimum experiment that showcase a bell shape. Relative areas were computed in reference to the initial peak area of carbamazepine and normalized with respect to multiple QC pooled samples. Error bars correspond to the standard deviation across replicate experiments.

wastewater treatment. In particular, this work has focused on simple water matrices containing carbamazepine (CBZ) at previously reported trace concentrations, for which the degradation was carried out in several scenarios with lower energy and chemicals requirement than in most studies. In fact, current densities lower than 50 A m^{-2} and sulfate concentrations similar to those found in wastewater effluents (1–10 mM) were used. In view of future scale-up opportunities, both these features represent a competitive advantage over other treatment technologies. Firstly, because electrochemical oxidation is considered one of the most environmentally-friendly AOPs [61], and the use of renewable energy can reduce its environmental impact by over 90% across multiple Life Cycle Assessment categories [62]. Secondly, because it is possible to degrade CBZ without the addition of chemical precursors, given that the ionic species required for the generation of oxidative radicals are typically already present in the wastewater. As a result, additional economic burdens as well as the formation of secondary waste streams can be circumvented.
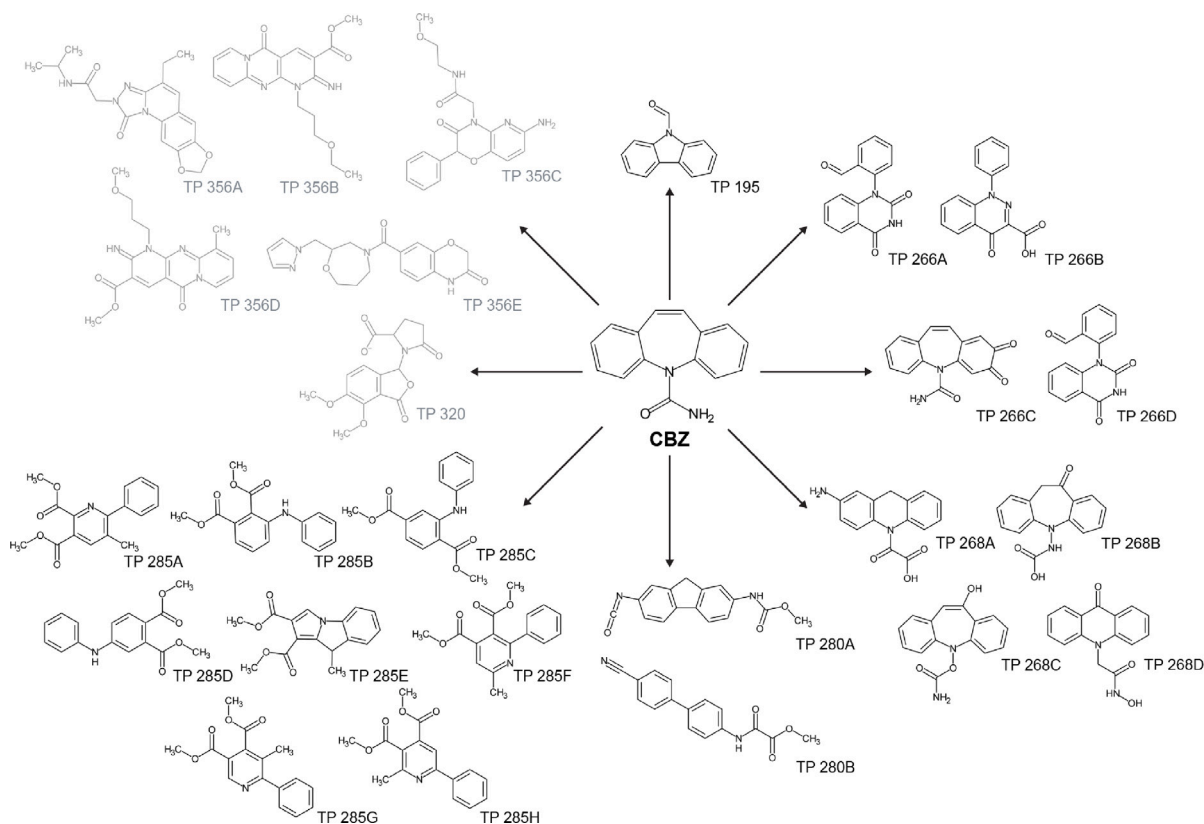
Fig. 13. Proposed chemical structures for the detected CBZ degradation products during the Taguchi optimum experiment. Structures drawn in darker font correspond to those meeting all selection criteria.

Table 3
Detailed information on detected CBZ degradation products during the Taguchi optimum experiment and their proposed structures. When more than one structure could be applicable to the same transformation product, they have been denoted with a letter A–H.

Exact mass (g mol^{-1})	m/z	RT (min)	Formula	Proposed chemical structure (s)	Match in the literature	Mass accuracy (ppm)
195.0687	196.0758	12.06	$C_{13}H_9NO$	TP 195	–	–
266.0696	267.0769	10.77	$C_{15}H_{10}N_2O_3$	TP 266A, TP 266B	1-(2-Formylphenyl) quinazoline-2,4(1H,3H)-dione [14,57–60]	1.73
266.0698	267.0769	8.21	$C_{15}H_{10}N_2O_3$	TP 266C, TP 266D	–	–
268.0857	269.0927	11.11	$C_{15}H_{12}N_2O_3$	TP 268A, TP 268B, TP 268C, TP 268D	–	–
280.0859	281.0925	13.28	$C_{16}H_{12}N_2O_3$	TP 280A, TP 280B	–	–
285.1009	286.1077	17.73	$C_{16}H_{15}NO_4$	TP 285A, TP 285B, TP 285C, TP 285D, TP 285E, TP 285F, TP 285G, TP 285H	–	–
311.0544	334.0438	12.02	–	–	–	–
320.0778	321.0850	11.86	$C_{15}H_{14}NO_7$	TP 320	–	–
325.0704	348.0595	12.50	–	–	–	–
356.1489	357.1563	11.88	$C_{18}H_{20}N_4O_4$	TP 356A, TP 356B, TP 356C, TP 356D, TP 356E	–	–

However, industrial implementation of these experimental conditions for CBZ degradation is strongly limited to the variability of the influent water matrix, especially if organic (e.g., dissolved organic matter, humic acids, amino acids, proteins...) and inorganic (e.g., (bi)carbonates, chlorides, bromides...) radical scavengers are present. These scavengers may not only hinder the overall process performance, but also lead to reaction intermediates or by-products that are more toxic than the original parent compound. For instance, it has been reported that the presence of active chlorine in an electrochemical oxidation system may lead to the formation and accumulation of toxic chlorate, perchlorate, chloramines and organochloride derivatives [63,

64]. Similarly, the formation of several organosulfates of concerning effects, such as phenyl sulfate and p-cresyl sulfate, has been recently reported as a result of direct radical addition mechanisms [65]. Moreover, it is also necessary to investigate the degradation of multiple CECs simultaneously, as in a real-case scenario they will be treated in a mixture and thus there will be different implications in terms of degradation efficiency, underlying kinetics, operational costs and toxicity risk estimations. Typically, CECs removal efficiencies decrease with increasing water matrix complexity, as more non-targeted species may participate in competitive reactions [22,45]. Nonetheless, some studies have also reported that water matrix constituents may in contrast have

neutral or promoting effects, depending on the reaction mechanisms taking place [45,46]. Thus, it is of utmost importance to evaluate water matrix effects depending on the wastewater and CECs of interest.

4. Conclusions

The Taguchi Method enabled the simultaneous optimization of multiple operating parameters, leading to the complete degradation of CBZ in less than 5 min under the optimal conditions of pH 2, 30 °C, 10 mM Na_2SO_4 anolyte, 1 µM initial CBZ and 50 A m^{-2}. Nonetheless, it was observed that the wastewater under treatment showed a natural tendency to evolve towards acidic conditions regardless of the initial pH and that the optimal conditions were due to the joint effect of having both SO_4^{2-} and NO_3^- ions in solution. Thus, the optimal results were also attained when replacing HNO_3 by $NaNO_3$, which alleviated the drawbacks of adjusting the pH before treatment. Complementary scenarios with different ion species, energy sources and current densities further corroborated the suitability of the optimum. In addition, the transformation products formed under the optimal conditions were evaluated. A total of 10 primary transformation products were detected and 8 of them were tentatively identified. A key finding was that these compounds were also eliminated in parallel to the removal of CBZ.

The contribution of different radicals in a sulfate-based medium was investigated through scavenging tests, which revealed that $^\bullet OH$ radicals are the dominant oxidative species. This phenomenon was for the first time linked to the Oxygen Evolution Reaction (OER), where at low potential, $HO_2^\bullet$ radicals and non-oxidized water molecules appear to be determinant factors for the scavenging of $SO_4^{\bullet-}$ radicals. In contrast, at high potential, even if $^\bullet OH$ radicals are abundant, the complete oxidation of the sulfate anolyte promotes oxidative species such as $SO_4^{\bullet-}$ and $S_2O_8^{\bullet-}$ radicals, which may also contribute to the pollutant degradation. Given the complexity of a non-scavenged scenario, the type, source and contribution of the radicals participating in the degradation of CBZ need to be further elucidated.

Declaration of competing interest

The authors declare that they have no known competing financial interests or personal relationships that could have appeared to influence the work reported in this paper.

Acknowledgments

Appendix A. Supplementary data

Supplementary material related to this article can be found online at https://doi.org/10.1016/j.cej.2022.137114.

References

[1] N.H. Tran, M. Reinhard, K.Y.-H. Gin, Occurrence and fate of emerging contaminants in municipal wastewater treatment plants from different geographical regions - A review, Water Res. 133 (2018) 182–207, http://dx.doi.org/10.1016/j.watres.2017.12.029.

[2] A.R. Ribeiro, O.C. Nunes, M.F.R. Pereira, A.M.T. Silva, An overview on the advanced oxidation processes applied for the treatment of water pollutants defined in the recently launched directive 2013/39/EU, Environ. Int. 75 (2015) 33–51, http://dx.doi.org/10.1016/j.envint.2014.10.027.

[3] M.A. Oturan, J.-J. Aaron, Advanced oxidation processes in water/wastewater treatment: Principles and applications. A review, Crit. Rev. Environ. Sci. Technol. 44 (23) (2014) 2577–2641, http://dx.doi.org/10.1080/10643389.2013.829765.

[4] R. Dewil, D. Mantzavinos, I. Poulios, M.A. Rodrigo, New perspectives for advanced oxidation processes, J. Environ. Manag. 195 (2017) 93–99, http://dx.doi.org/10.1016/j.jenvman.2017.04.010.

[5] D.B. Miklos, C. Remy, M. Jekel, K.G. Linden, J.E. Drewes, U. Hübner, Evaluation of advanced oxidation processes for water and wastewater treatment - A critical review, Water Res. 139 (2018) 118–131, http://dx.doi.org/10.1016/j.watres.2018.03.042.

[6] S. Giannakis, K.Y.A. Lin, F. Ghanbari, A review of the recent advances on the treatment of industrial wastewaters by sulfate radical-based advanced oxidation processes (SR-AOPs), Chem. Eng. J. 406 (2021) http://dx.doi.org/10.1016/j.cej.2020.127083.

[7] U. Ushani, X. Lu, J. Wang, Z. Zhang, J. Dai, Y. Tan, S. Wang, W. Li, C. Niu, T. Cai, N. Wang, G. Zhen, Sulfate radicals-based advanced oxidation technology in various environmental remediation: A state-of-the-art review, Chem. Eng. J. 402 (2020) http://dx.doi.org/10.1016/j.cej.2020.126232.

[8] P. Devi, U. Das, A.K. Dalai, In-situ chemical oxidation: Principle and applications of peroxide and persulfate treatments in wastewater systems, Sci. Total Environ. 571 (2016) 643–657, http://dx.doi.org/10.1016/j.scitotenv.2016.07.032.

[9] A. Farhat, J. Keller, S. Tait, J. Radjenovic, Assessment of the impact of chloride on the formation of chlorinated by-products in the presence and absence of electrochemically activated sulfate, Chem. Eng. J. 330 (2017) 1265–1271, http://dx.doi.org/10.1016/j.cej.2017.08.033.

[10] S. Guerra-Rodríguez, E. Rodríguez, D.N. Singh, J. Rodríguez-Chueca, Assessment of sulfate radical-based advanced oxidation processes for water and wastewater treatment: A review, Water 10 (12) (2018) http://dx.doi.org/10.3390/w10121828.

[11] T. Tang, G. Lu, R. Wang, Z. Qiu, K. Huang, W. Lian, X. Tao, Z. Dang, H. Yin, Rate constants for the reaction of hydroxyl and sulfate radicals with organophosphorus esters (OPEs) determined by competition method, Ecotoxicol Environ. Safety 170 (2019) 300–305, http://dx.doi.org/10.1016/j.ecoenv.2018.11.142.

[12] X. Duan, S. Yang, S. Wacławek, G. Fang, R. Xiao, D.D. Dionysiou, Limitations and prospects of sulfate radical-based advanced oxidation processes, J. Environ. Chem. Eng. 8 (4) (2020) 103849, http://dx.doi.org/10.1016/j.jece.2020.103849.

[13] J. Radjenovic, M. Petrovic, Removal of sulfamethoxazole by electrochemically activated sulfate: Implications of chloride addition, J. Hazard. Mater. 333 (2017) 242–249, http://dx.doi.org/10.1016/j.jhazmat.2017.03.040.

[14] H. Song, L. Yan, J. Jiang, J. Ma, Z. Zhang, J. Zhang, P. Liu, T. Yang, Electrochemical activation of persulfates at BDD anode: Radical or nonradical oxidation? Water Res. 128 (2018) 393–401, http://dx.doi.org/10.1016/j.watres.2017.10.018.

[15] L. Chen, C. Lei, Z. Li, B. Yang, X. Zhang, L. Lei, Electrochemical activation of sulfate by BDD anode in basic medium for efficient removal of organic pollutants, Chemosphere 210 (2018) 516–523, http://dx.doi.org/10.1016/j.chemosphere.2018.07.043.

[16] I. Sirés, E. Brillas, M.A. Oturan, M.A. Rodrigo, M. Panizza, Electrochemical advanced oxidation processes: Today and tomorrow. A review, Environ. Sci. Pollut. Res. 21 (2014) 8336–8367, http://dx.doi.org/10.1007/s11356-014-2783-1.

[17] D. Seibert, C.F. Zorzo, F.H. Borba, R.M. de Souza, H.B. Quesada, R. Bergamasco, A.T. Baptista, J.J. Inticher, Occurrence, statutory guideline values and removal of contaminants of emerging concern by electrochemical advanced oxidation processes: A review, Sci. Total Environ. 748 (2020) 141527, http://dx.doi.org/10.1016/j.scitotenv.2020.141527.

[18] S. Garcia-Segura, J.D. Ocon, M.N. Chong, Electrochemical oxidation remediation of real wastewater effluents - A review, Process Saf. Environ. Prot. 113 (2018) 48–67, http://dx.doi.org/10.1016/j.psep.2017.09.014.

[19] J.V. Macpherson, A practical guide to using boron doped diamond in electrochemical research, Phys. Chem. Chem. Phys. 17 (2015) 2935–2949, http://dx.doi.org/10.1039/c4cp04022h.

[20] X. Chen, G. Chen, F. Gao, P.L. Yue, High-performance Ti/BDD electrodes for pollutant oxidation, Environ. Sci. Technol. 37 (21) (2003) 5021–5026, http://dx.doi.org/10.1021/es026443f.

[21] J. Ryl, L. Burczyk, R. Bogdanowicz, M. Sobaszek, K. Darowicki, Study on surface termination of boron-doped diamond electrodes under anodic polarization in H_2SO_4 by means of dynamic impedance technique, Carbon 96 (2016) 1093–1105, http://dx.doi.org/10.1016/j.carbon.2015.10.064.

[22] G. Divyapriya, P.V. Nidheesh, Electrochemically generated sulfate radicals by boron doped diamond and its environmental applications, Curr. Opin. Solid State Mater. Sci. 25 (3) (2021) 100921, http://dx.doi.org/10.1016/j.cossms.2021.100921.

[23] C.A. Martínez-Huitle, S. Ferro, Electrochemical oxidation of organic pollutants for the wastewater treatment: Direct and indirect processes, Chem. Soc. Rev. 35 (12) (2006) 1324–1340, http://dx.doi.org/10.1039/B517632H.

[24] A. Farhat, J. Keller, S. Tait, J. Radjenovic, Oxidative capacitance of sulfate-based boron-doped diamond electrochemical system, Electrochem. Commun. 89 (2018) 14–18, http://dx.doi.org/10.1016/j.elecom.2018.02.007.

[25] A. Farhat, J. Keller, S. Tait, J. Radjenovic, Removal of persistent organic contaminants by electrochemically activated sulfate, Environ. Sci. Technol. 49 (2015) 14326–14333, http://dx.doi.org/10.1021/acs.est.5b02705.

[26] Y. Zhang, S.-U. Geißen, C. Gal, Carbamazepine and diclofenac: Removal in wastewater treatment plants and occurrence in water bodies, Chemosphere 73 (8) (2008) 1151–1161, http://dx.doi.org/10.1016/j.chemosphere.2008.07.086.

[27] D.P. Mohapatra, S.K. Brar, R.D. Tyagi, P. Picard, R.Y. Surampalli, Analysis and advanced oxidation treatment of a persistent pharmaceutical compound in wastewater and wastewater sludge-carbamazepine, Sci. Total Environ. 470–471 (2014) 58–75, http://dx.doi.org/10.1016/j.scitotenv.2013.09.034.

[28] J. Wang, S. Wang, Reactive species in advanced oxidation processes: Formation, identification and reaction mechanism, Chem. Eng. J. 401 (2020) 126158, http://dx.doi.org/10.1016/j.cej.2020.126158.

[29] NORMAN-Network, NORMAN database system, 2021, https://www.norman-network.com/nds/.

[30] C. Teodosiu, A.-F. Gilca, G. Barjoveanu, S. Fiore, Emerging pollutants removal through advanced drinking water treatment: A review on processes and environmental performances assessment, J. Clean. Prod. 197 (2018) 1210–1221, http://dx.doi.org/10.1016/j.jclepro.2018.06.247.

[31] J. Radjenovic, M. Petrovic, Sulfate-mediated electrooxidation of X-ray contrast media on boron-doped diamond anode, Water Res. 94 (2016) 128–135, http://dx.doi.org/10.1016/j.watres.2016.02.045.

[32] X. Yu, Z. Gocze, D. Cabooter, R. Dewil, Efficient reduction of carbamazepine using UV-activated sulfite: Assessment of critical process parameters and elucidation of radicals involved, Chem. Eng. J. 404 (2021) http://dx.doi.org/10.1016/j.cej.2020.126403.

[33] R. Core Team, R: A Language and Environment for Statistical Computing, R Foundation for Statistical Computing, Vienna, Austria, 2021, URL https://www.R-project.org/.

[34] Z. Pang, J. Chong, G. Zhou, D.A. de Lima Morais, L. Chang, M. Barrette, C. Gauthier, P.-E. Jacques, S. Li, J. Xia, MetaboAnalyst 5.0: NArrowing the gap between raw spectra and functional insights, Nucleic Acids Res. 49 (W1) (2021) W388–W396, http://dx.doi.org/10.1093/nar/gkab382.

[35] C. Ruttkies, E.L. Schymanski, S. Wolf, J. Hollender, S. Neumann, MetFrag Relaunched: Incorporating strategies beyond in silico fragmentation, J. Cheminformatics 8 (1) (2016) 1–16, http://dx.doi.org/10.1186/s13321-016-0115-9.

[36] ChemAxon, Marvin 17.21.0, ChemAxon, 2021, URL https://www.chemaxon.com.

[37] L. Rizzo, S. Malato, D. Antakyali, V.G. Beretsou, M.B. Dolić, W. Gernjak, E. Heath, I. Ivancev-Tumbas, P. Karaolia, A.R. Lado Ribeiro, G. Mascolo, C.S. McArdell, H. Schaar, A.M.T. Silva, D. Fatta-Kassinos, Consolidated vs new advanced treatment methods for the removal of contaminants of emerging concern from urban wastewater, Sci. Total Environ. 655 (2019) 986–1008, http://dx.doi.org/10.1016/j.scitotenv.2018.11.265.

[38] S. Periyasamy, X. Lin, S.O. Ganiyu, S.-K. Kamaraj, A. Thiam, D. Liu, Insight into BDD electrochemical oxidation of florfenicol in water: Kinetics, reaction mechanism, and toxicity, Chemosphere 288 (2022) 132433, http://dx.doi.org/10.1016/j.chemosphere.2021.132433.

[39] L. Varanasi, E. Coscarelli, M. Khaksari, L.R. Mazzoleni, D. Minakata, Transformations of dissolved organic matter induced by UV photolysis, hydroxyl radicals, chlorine radicals, and sulfate radicals in aqueous-phase UV-Based advanced oxidation processes, Water Res. 135 (2018) 22–30, http://dx.doi.org/10.1016/j.watres.2018.02.015.

[40] K. Gurung, M.C. Ncibi, M. Shestakova, M. Sillanpää, Removal of carbamazepine from MBR effluent by electrochemical oxidation (EO) using a $Ti/Ta_2O_5-SnO_2$ electrode, Appl. Catal. B 221 (2018) 329–338, http://dx.doi.org/10.1016/j.apcatb.2017.09.017.

[41] S. Yang, P. Wang, X. Yang, L. Shan, W. Zhang, X. Shao, R. Niu, Degradation efficiencies of azo dye acid orange 7 by the interaction of heat, UV and anions with common oxidants: Persulfate, peroxymonosulfate and hydrogen peroxide, J. Hazard. Mater. 179 (1) (2010) 552–558, http://dx.doi.org/10.1016/j.jhazmat.2010.03.039.

[42] S. Hadi, E. Taheri, M.M. Amin, A. Fatehizadeh, T.M. Aminabhavi, Advanced oxidation of 4-chlorophenol via combined pulsed light and sulfate radicals methods: Effect of co-existing anions, J. Environ. Manag. 291 (2021) 112595, http://dx.doi.org/10.1016/j.jenvman.2021.112595.

[43] G. Acosta-Santoyo, L.F. León-Fernández, E. Bustos, P. Cañizares, M.A. Rodrigo, J. Llanos, On the production of ozone, hydrogen peroxide and peroxone in pressurized undivided electrochemical cells, Electrochim. Acta 390 (2021) 138878, http://dx.doi.org/10.1016/j.electacta.2021.138878.

[44] S.C. Perry, D. Pangotra, L. Vieira, L.-I. Csepei, V. Sieber, L. Wang, C.P. de León, F.C. Walsh, Electrochemical synthesis of hydrogen peroxide from water and oxygen, Nat. Rev. Chem. 3 (7) (2019) 442–458, http://dx.doi.org/10.1038/s41570-019-0110-6.

[45] A.R. Lado Ribeiro, N.F.F. Moreira, G. Li Puma, A.M.T. Silva, Impact of water matrix on the removal of micropollutants by advanced oxidation technologies, Chem. Eng. J. 363 (2019) 155–173, http://dx.doi.org/10.1016/j.cej.2019.01.080.

[46] Y. Wang, F.A. Roddick, L. Fan, Direct and indirect photolysis of seven micropollutants in secondary effluent from a wastewater lagoon, Chemosphere 185 (2017) 297–308, http://dx.doi.org/10.1016/j.chemosphere.2017.06.122.

[47] S.O. Ganiyu, S. Sable, M.G. El-Din, Advanced oxidation processes for the degradation of dissolved organics in produced water: A review of process performance, degradation kinetics and pathway, Chem. Eng. J. (2021) 132492, http://dx.doi.org/10.1016/j.cej.2021.132492.

[48] H. Milh, D. Cabooter, R. Dewil, Role of process parameters in the degradation of sulfamethoxazole by heat-activated peroxymonosulfate oxidation: Radical identification and elucidation of the degradation mechanism, Chem. Eng. J. 422 (2021) 130457, http://dx.doi.org/10.1016/j.cej.2021.130457.

[49] I. Kisacik, A. Stefanova, S. Ernst, H. Baltruschat, Oxidation of carbon monoxide, hydrogen peroxide and water at a boron doped diamond electrode: The competition for hydroxyl radicals, Phys. Chem. Chem. Phys. 15 (2013) 4616–4624, http://dx.doi.org/10.1039/C3CP44643C.

[50] S. Wang, J. Wang, Degradation of carbamazepine by radiation-induced activation of peroxymonosulfate, Chem. Eng. J. 336 (2018) 595–601, http://dx.doi.org/10.1016/j.cej.2017.12.068.

[51] J. Wang, S. Wang, Activation of persulfate (PS) and peroxymonosulfate (PMS) and application for the degradation of emerging contaminants, Chem. Eng. J. 334 (2018) 1502–1517, http://dx.doi.org/10.1016/j.cej.2017.11.059.

[52] S.W. da Silva, J. Wang, M.A.S. Rodrigues, A.M. Bernardes, V. Pérez-Herranz, Using p-Si/BDD anode for the electrochemical oxidation of norfloxacin, J. Electroanal. Chem. 832 (2019) 112–120, http://dx.doi.org/10.1016/j.jelechem.2018.10.049.

[53] J.P. d. P. Barreto, K.C. d. F. Araujo, D.M. de Araujo, C.A. Martinez-Huitle, Effect of sp^3/sp^2 ratio on boron doped diamond films for producing persulfate, ECS Electrochem. Lett. 4 (12) (2015) 9–11, http://dx.doi.org/10.1149/2.0061512eel.

[54] W. Chu, Y.R. Wang, H.F. Leung, Synergy of sulfate and hydroxyl radicals in $UV/S_2O_8^{2-}/H_2O_2$ oxidation of iodinated X-ray contrast medium iopromide, Chem. Eng. J. 178 (2011) 154–160, http://dx.doi.org/10.1016/j.cej.2011.10.033.

[55] C.-W. Wang, C. Liang, Oxidative degradation of TMAH solution with UV persulfate activation, Chem. Eng. J. 254 (2014) 472–478, http://dx.doi.org/10.1016/j.cej.2014.05.116.

[56] M.R. Dalman, A. Deeter, G. Nimishakavi, Z.-H. Duan, Fold change and p-value cutoffs significantly alter microarray interpretations, BMC Bioinformatics 13 (2) (2012) 1–4.

[57] Y.F. Rao, L. Qu, H. Yang, W. Chu, Degradation of carbamazepine by Fe(II)-activated persulfate process, J. Hazard. Mater. 268 (2014) 23–32, http://dx.doi.org/10.1016/j.jhazmat.2014.01.010.

[58] Y.F. Rao, W. Chu, Y.R. Wang, Photocatalytic oxidation of carbamazepine in triclinic-WO_3 suspension: Role of alcohol and sulfate radicals in the degradation pathway, Appl. Catal. A 468 (2013) 240–249, http://dx.doi.org/10.1016/j.apcata.2013.08.050.

[59] W. Gebhardt, H.F. Schröder, Liquid chromatography–(tandem) mass spectrometry for the follow-up of the elimination of persistent pharmaceuticals during wastewater treatment applying biological wastewater treatment and advanced oxidation, J. Chromatogr. A 1160 (1) (2007) 34–43, http://dx.doi.org/10.1016/j.chroma.2007.05.075.

[60] D.C. McDowell, M.M. Huber, M. Wagner, U. Von Gunten, T.A. Ternes, Ozonation of carbamazepine in drinking water: Identification and kinetic study of major oxidation products, Environ. Sci. Technol. 39 (20) (2005) 8014–8022, http://dx.doi.org/10.1021/es050043l.

[61] E. Chatzisymeon, S. Foteinis, D. Mantzavinos, T. Tsoutsos, Life cycle assessment of advanced oxidation processes for olive mill wastewater treatment, J. Clean. Prod. 54 (2013) 229–234, http://dx.doi.org/10.1016/j.jclepro.2013.05.013.

[62] I. Muñoz, J. Rieradevall, F. Torrades, J. Peral, X. Domènech, Environmental assessment of different solar driven advanced oxidation processes, Sol. Energy 79 (4) (2005) 369–375, http://dx.doi.org/10.1016/j.solener.2005.02.014.

[63] S. Garcia-Segura, J. Keller, E. Brillas, J. Radjenovic, Removal of organic contaminants from secondary effluent by anodic oxidation with a boron-doped diamond anode as tertiary treatment, J. Hazard. Mater. 283 (2015) 551–557, http://dx.doi.org/10.1016/j.jhazmat.2014.10.003.

[64] J.D. García-Espinoza, P. Miajaylova-Nacheva, M. Avilés-Flores, Electrochemical carbamazepine degradation: Effect of the generated active chlorine, transformation pathways and toxicity, Chemosphere 192 (2018) 142–151, http://dx.doi.org/10.1016/j.chemosphere.2017.10.147.

[65] J. Van Buren, A.A. Cuthbertson, D. Ocasio, D.L. Sedlak, Ubiquitous production of organosulfates during treatment of organic contaminants with sulfate radicals, Environ. Sci. Technol. Lett. 8 (7) (2021) 574–580, http://dx.doi.org/10.1021/acs.estlett.1c00316.